Symmetric Current-Balancing Circuit for LED Backlight With Dimming

Sungjin Choi, *Member, IEEE*, and Taehoon Kim

***Abstract*—One of the key challenges in driving multiple light-emitting-diode (LED) strings for a liquid-crystal-display (LCD) backlight system is to ensure uniform current control. Unequal current sharing between the strings is due to manufacturing spread and temperature variations. In this paper, a novel current-balancing circuit for LED backlights is proposed. A smart combination of an inherent symmetry of circuit and capacitive balancing mechanism enables an efficient and cost-effective current balancing. The operating principle of the proposed method is analyzed, and an appealing generalization is made. The feasibility of the proposed scheme is verified by developing a hardware prototype with a dimming feature to drive a 100-W edge-type backlight system, having six LED strings for a large-scale LCD panel.**

***Index Terms*—Backlight, current balancing, light-emitting-diode (LED) driver, liquid crystal display (LCD).**

I. Introduction

WITH SIGNIFICANT progress in the liquid-crystal-display (LCD) flat-panel display industry, efficient and cost-effective backlight driver circuits have gained the much needed attention in power electronics industry. As the size of LCD panels increases, more backlight sources should be installed to provide required brightness in the display device. Recently, low-voltage dc backlight sources such as light-emitting-diode (LED) strings (or series-connected white LED arrays) are rapidly substituting high-voltage ac light sources such as cold cathode fluorescent lamps because of its long lifetime, safety, and eco-friendly nature. Fig. 1(a) shows a typical large-scale LCD backlight system called edge-type configuration. Six LED strings are placed in the edge of the LCD panel, and each string has multiple series-connected white LED chips.

In this application, brightness uniformity in LCD backlights is the most important performance factor and maintaining the uniform current distribution between backlight sources is the primary function of the drive circuit. As for LED backlights, because the dc waveform is needed, extensive research works mostly have been dedicated to active balancing methods such as the linear balancing method [4] or dedicated dc/dc converters [5]. There have been some previous reports [6], [7], which tried to combine both methods and apply active control to improve current uniformity. Over the last few years, IC vendors have integrated these dc-balancing functions into a single chip to reduce the cost but the overall implementation is still expensive [8], [9].

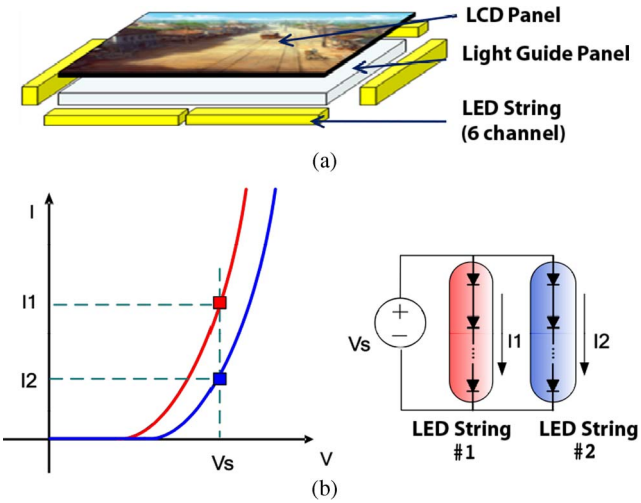

Fig. 1. LED backlight system and current imbalance problem.

In this paper, a new dc-balancing circuit for LED strings in backlight systems is proposed and dimming control has been added to the previous work [11]. The suggested scheme is a simple, efficient, and cost-effective solution because it utilizes an inherent symmetric balancing feature only using reactive components and diode rectifier.

II. Conventional Balancing Method

In LED strings, the forward voltage and current are exponentially related—i.e., even when the forward voltage changes slightly, its current varies dramatically. In reality, even LEDs from the same production lot have poorly matched I–V characteristics, as in Fig. 1(b). When constructing a system where multiple LED strings are driven by a single drive circuit, this mismatch causes the LEDs not to share the current equally. Without a balancing mechanism, LED current can be severely unbalanced even if energized by the same voltage. If the current values are different, their luminous intensity is not uniform and the color spectrum can be shifted from the desired value [12]–[14]. A LED used in this manner may also cause thermal runaway and damage the device itself.

To solve this problem, a resistor can be placed in series with each LED to minimize current differences, as shown in [15]. However, this method cannot balance the circuit without

Manuscript received September 30, 2010; revised February 8, 2011; accepted March 15, 2011. Date of publication April 5, 2011; date of current version November 1, 2011.

S. Choi is with the School of Electrical Engineering, University of Ulsan, Ulsan 680-749, Korea (e-mail: sjchoi@ulsan.ac.kr).

T. Kim is with the Advanced R&D Group, Visual Display Division, Samsung Electronics Company, Ltd., Suwon 443-742, Korea (e-mail: funnydie@naver.com)

Color versions of one or more of the figures in this paper are available online at http://ieeexplore.ieee.org.

Digital Object Identifier 10.1109/TIE.2011.2138112

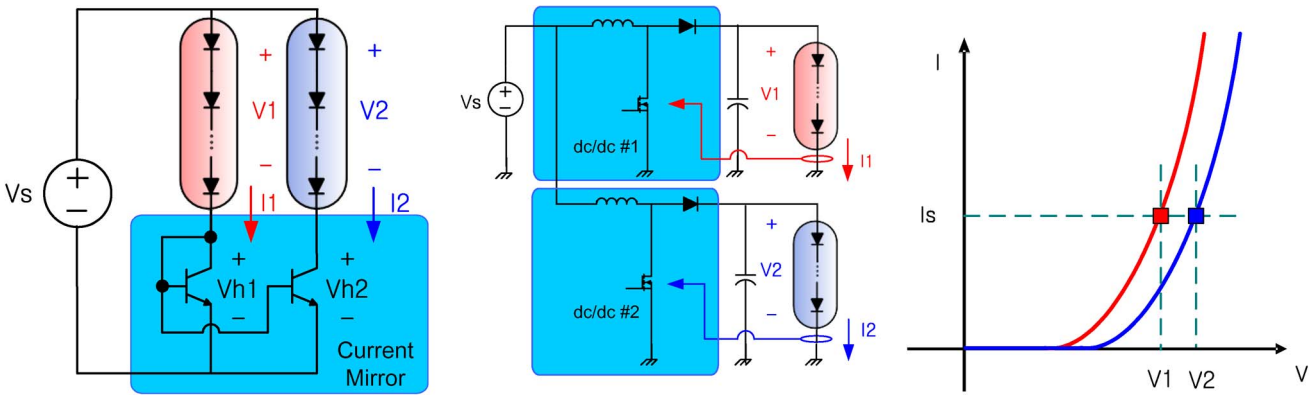

Fig. 2. Conventional method. (a) Linear current mirror. (b) Dedicated dc/dc converter. (c) I–V curves in both methods.

dissipating significant loss in the balancing resistors. More reasonable approaches can be categorized by the following two methods: a linear regulator method and a switching regulator method.

A. Linear Current-Mirror Regulator Method

To equalize the currents in each LED string, the current-mirror-based linear regulator method, shown in Fig. 2(a), is very widely used. In this driving method, the load current is balanced by a β gain of transistor switches and each transistor makes a nearly equal current in each LED string. With the same voltage source, the transistor forces a different operating voltage and the voltage difference between the supply voltage and the operating voltage of the string, V1 or V2, is applied to individual transistors. This extra voltage, called "headroom voltage," causes a serious power loss, which is given by load current multiplied by the voltage. The power dissipation can take a large portion of the circuit loss either by higher current or large deviation of the operating voltage between the LED. Because of this kind of driver loss, this approach is only suitable for the LED string with a small number of series connections of LED chips. When the number of the series connections is larger, or a large power is required, another method should be adopted.

B. Dedicated DC/DC Converter Method

To reduce the power dissipation of the balancing circuit, a separate voltage source can be used. In this method, the number of dc–dc converters equals to the number of LED strings. The current in each LED string is sensed, and its individual feedback controller maintains the output voltage to equalize the current, as shown in Fig. 2(b). On the I–V curve, the load condition is maintained by different voltages, V1 and V2, to each LED string. Each converter is designed optimally, and its efficiency is much higher than the linear regulator method. However, the circuit is complex and far more expensive.

C. Reactive Balancing Method

To reduce circuit cost and power loss simultaneously, the adoption of reactive balancing techniques used in ac light source [1]–[3] has been investigated. Recently, a capacitive balance scheme was proposed for paralleled high-flux LEDs [10], which allows current flow in an alternating manner with LEDs placed in sets of antiparallel branches. However, it provides half-wave rectified sine LED currents and is not directly applicable to LED backlight systems. In this paper, as an enhancement of [11], the capacitive balancing method was further investigated and completely merged into a new LED backlight driver circuit with dc driving and dimming features.

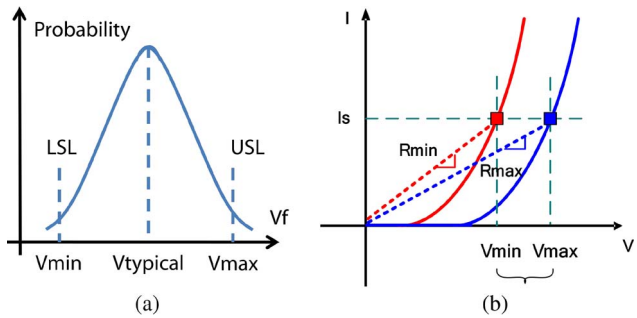

Fig. 3. Manufacturing spread in forward voltage and dc load impedance.

III. Theory of Reactive Balancing for DC Loads

A. Modeling of LED Strings

As shown in Fig. 3(a), in mass production, LED shows manufacturing spread in its forward voltage due to statistical distribution. The forward voltage is also dependent on the operating temperature. LED vendors usually specify the forward voltage as an upper specification limit and a lower specification limit in a constant bias current and in a specified operating temperature. In the sense of bias point calculation in the following circuit operation analysis, dc equivalent resistance for a LED string can be defined as the ratio of the operating forward voltage to the bias current, as in Fig. 3(b). The maximum and the minimum load resistance values, namely, $R_{\max}$ and $R_{\min}$, are calculated from datasheets, and the LED strings can be regarded as resistance loads with values between the two resistance values.

B. Capacitive Balancing for Paralleled DC Loads

Two slightly different dc loads, $R1$ and $R2$, for example, can be balanced by placing a lossless reactive component instead of

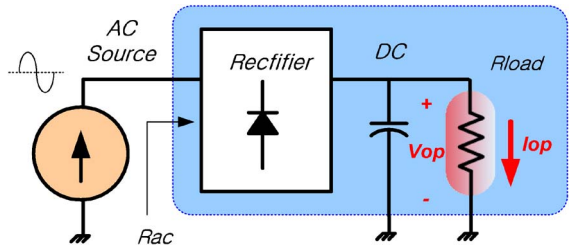

Fig. 4. AC equivalent resistance including rectifier and dc load.

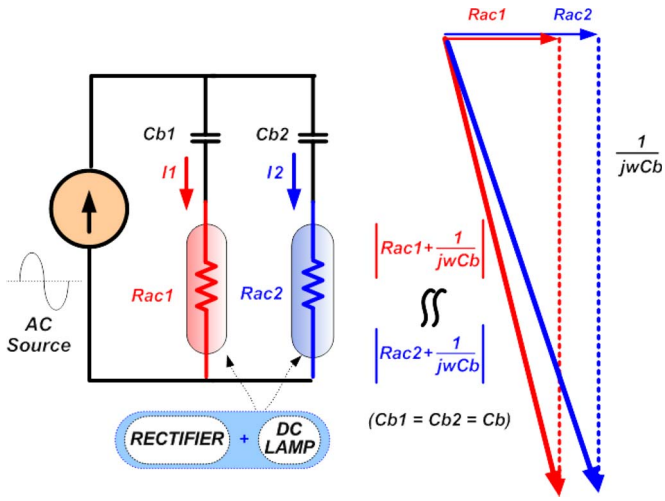

Fig. 5. Reactive balancing for the rectifier-driven load.

a lossy series balancing resistance. However, to utilize reactive impedance balancing, the dc load should be driven by an ac source coupled with a diode rectifier. The diode rectifier including the load can also be modeled by an ac equivalent resistance $R_{\rm ac}$ by using energy balance [16] (Fig. 4). The basic idea is to achieve dc balancing by using ac impedance balancing first and then rectify and filter the ac waveforms to a pure dc value. This paper adopts the capacitive balancing scheme to obtain ac reactive impedance.

As shown in Fig. 5, the current balancing can be achieved by balancing capacitors and the current in each branch can be obtained as in (1) below. The impedance vector diagram shows that the ac current in each equivalent resistance is almost the same if the reactance of C_b is sufficiently larger than the load resistance itself

$$\frac{I_2}{I_1} = \frac{1/(j\omega C_{b1}) + R_{\rm ac1}}{1/(j\omega C_{b2}) + R_{\rm ac2}}. \tag{1}$$

However, in real situations, the tolerance in the capacitance can also influence the balancing performance. Taking that factor into account, the errors in the current between the two branches can be estimated. If α is the tolerance rate of the balancing capacitors, which is normally 5%, and β is the tolerance of the load impedance, which is dependent on the load, the current deviation ratio can be calculated as in (3)

$$C_{b2} = C_{b1}(1 \pm \alpha) \quad R_{\rm ac2} = R_{\rm ac1}(1 \pm \beta) \tag{2}$$

$$D \equiv \frac{|I_1 - I_2|}{I_1} = \frac{\sqrt{\alpha^2 q^2 + \beta^2}}{\sqrt{q^2(1 \pm \alpha)^2 + (1 \pm \beta)^2}} \tag{3}$$

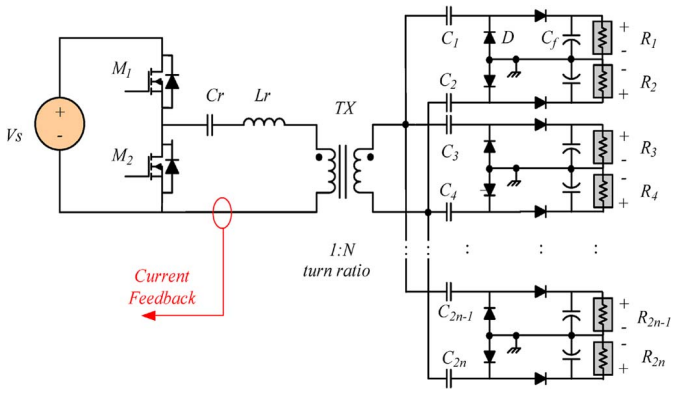

Fig. 6. Proposed symmetric current-balancing driver for multiple dc loads.

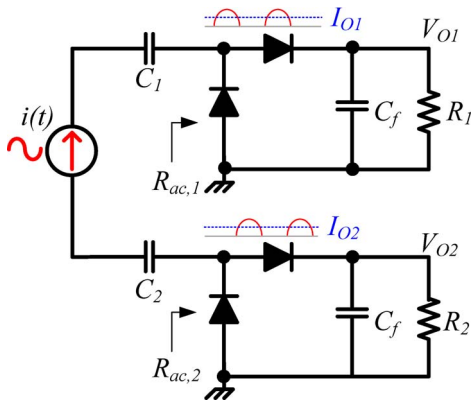

Fig. 7. Derivation of ac equivalent resistance.

where the reactance factor $q \equiv 1/(\omega C_{b1} R_{\rm ac1})$.

IV. Analysis of Principle of Operation

As a generalized implementation of the proposed balancing mechanism, Fig. 6 shows the symmetric current-balancing driver for $2n$ number of dc loads. The source side consists of a series resonant branch and half-bridge MOSFET switch pair and operates above the resonance frequency to supply a sinusoidal current to the secondary side. The secondary side consists of balancing capacitors, current-driven symmetric half-wave rectifiers, output filtering capacitors, and dc loads.

The operation of load current balancing is guided by the following three rules: 1) total current control; 2) symmetry of even and odd branches; and 3) capacitive impedance balancing mechanism.

A. Total Current Control

Instead of sensing the current in each branch, the current control loop regulates the total primary current such that the sum of the secondary-side current should be constant. Let the magnitude of the secondary sinusoidal current i_T be always constant as in the following analysis:

$$i_T(t) = I_T \sin(\omega t). \tag{4}$$

By applying fundamental harmonic approximation and an energy balance equation [16] to the simplified rectifier circuit

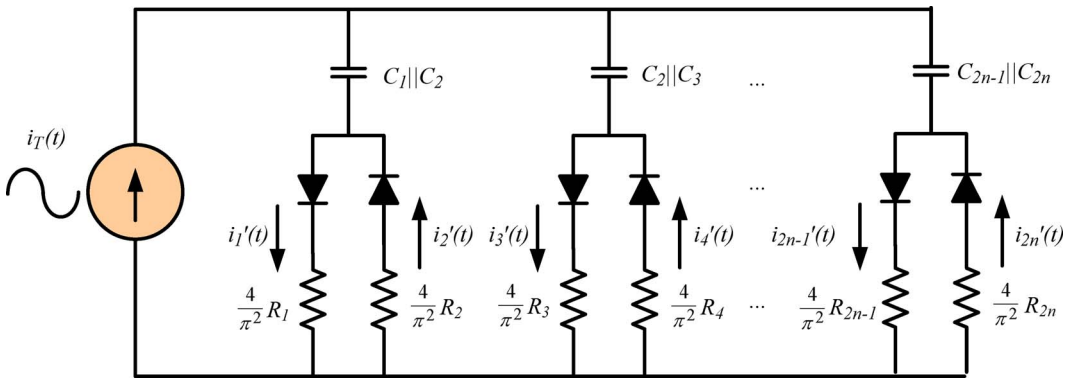

Fig. 8. AC equivalent model for the proposed circuit.

in Fig. 7, the ac equivalent resistance $R_{\mathrm{ac},k}$ is derived as (5) given that individual load resistance is R_k

$$R_{\mathrm{ac},k} = \frac{4}{\pi^2} R_k, \qquad k = 1, 2, \ldots, 2n. \tag{5}$$

B. Symmetry of Even and Odd Branches

From the aforementioned results, the overall equivalent circuit for the proposed circuit is shown in Fig. 8. The circuit has even/ odd symmetry in the sense that the odd branches are activated in the positive cycle of the source and the even parts are energized only in the negative cycle.

For the odd branch, the following current relation holds:

$$i_T(t) = \begin{cases} I_k' \sin(\omega t) & (0 \le \omega t < \pi) \\ 0 & (\pi \le \omega t < 2\pi) \end{cases} \tag{6}$$

where $k = 1, 3, 5, \ldots, (2n-1)$.

Similarly, for the even branch, the current is given by

$$i_T(t) = \begin{cases} 0 & (0 \le \omega t < \pi) \\ I_k' \sin(\omega t) & (\pi \le \omega t < 2\pi) \end{cases} \tag{7}$$

where $k = 2, 4, 6, \ldots, 2n$.

Applying again the energy balance equation in (7), the current on the ac side is related to the individual dc load current, as shown in (8), where I_k' is the magnitude of the current that flows in $R_{\mathrm{ac},k}$ and I_k is the magnitude of the current in R_k

$$I_k' = \pi I_k, \qquad k = 1, 2, \ldots, 2n. \tag{8}$$

Due to the inherent symmetry of the half-wave rectifier, the partial sum of the currents in the even branch and that of the currents in the odd branch have the same value as in

$$\sum_{k,\mathrm{odd}} I_k' = \sum_{k,\mathrm{even}} I_k' = I_T. \tag{9}$$

C. Capacitive Impedance Balancing Mechanism

As can be seen from the equivalent circuit, the slightly different ac loads $R_{\mathrm{ac},k}$ are balanced by series capacitors $C_{b,\mathrm{eff}}$ and the ac current in each equivalent resistance is almost the same if the impedance of $C_{b,\mathrm{eff}}$ is made sufficiently larger than the load resistance, thus meaning that the following holds:

$$\left|I_i' - I_j'\right| \to 0, \qquad \text{for even } i, j \text{ with } i \ne j \tag{10}$$

$$\left|I_i' - I_j'\right| \to 0, \qquad \text{for odd } i, j \text{ with } i \ne j. \tag{11}$$

From (9) to (11), all the dc load currents are balanced to have nearly the same value as in

$$\left|I_i' - I_j'\right| \to 0, \qquad \text{for } i, j = 1, 2, \ldots, 2n \text{ with } i \ne j. \tag{12}$$

Combining (12) with (8) verifies the balancing operation (13) of the proposed circuit

$$I_i \approx I_j \to \frac{I_T}{n\pi}, \qquad \text{for } i, j = 1, 2, \ldots, 2n \text{ with } i \ne j. \tag{13}$$

TABLE I
DATASHEET OF A LED STRING SAMPLE FOR A 46″ PANEL (LBU46MFAE7 BY SEMCO)

Symbol	Min	Typ	Max	Unit	Test condition (I_{op})
Vop	164.3	171	177.7	V	@ 95mA, 25°C

V. Design Procedure

To design the circuit, the dc load impedance R_{load} should be found from the datasheet. Most LED vendors specify the upper and lower limits for the operating forward voltage V_{op} in the operating current I_{op} at the specified temperature condition. Table I shows the forward voltage spread of the LED string sample (LBU46MFAE7 by SEMCO) used in this paper. The maximum and minimum equivalent dc impedances, namely, $R_{\mathrm{load,max}}$ and $R_{\mathrm{load,min}}$, can be calculated by

$$R_{\mathrm{load,max}} = \frac{V_{\mathrm{op,max}}}{I_{\mathrm{op}}} \quad R_{\mathrm{load,min}} = \frac{V_{\mathrm{op,min}}}{I_{\mathrm{op}}}. \tag{14}$$

To design the balancing network, the ac equivalent resistance R_{ac}, including the rectifier, is then calculated, assuming sinusoidal driving condition

$$R_{\mathrm{ac}} = \frac{4}{\pi^2} R_{\mathrm{load}}. \tag{15}$$

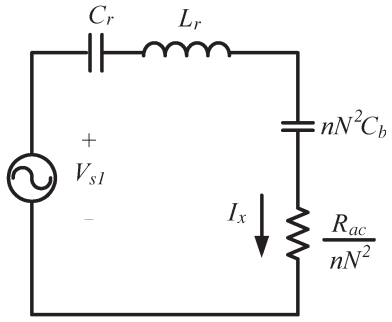

Fig. 9. Simplified circuit for the overall circuit.

For simplicity and without any loss of generality, it is assumed that the balancing components in Fig. 6 are designed with the same value as

$$C_1 = C_2 = \cdots = C_{2n} = 2C_b. \tag{16}$$

From the allowable deviation specification in the LED string currents which determines the overall brightness uniformity of the backlight unit, the required reactance factor q is calculated by (3). By choosing a relevant switching frequency ω, the effective balancing capacitor value C_b is calculated from the definition of the reactance factor.

To investigate the gain characteristics of the proposed converter, the simplified circuit in Fig. 9 has been derived from Fig. 6. In the meantime, all the components in the transformer secondary have been reflected to the primary side and all the $2n$ numbers of the identical balancing networks including rectifiers and loads are merged into equivalent components. This converter can be regarded as a series resonant network when applying fundamental frequency and high Q approximation of the resonant tank, as in (17) and (18); the resonant frequency and the loaded quality factor can be defined as in (19) and (20)

$$V_{s1}(t) = \frac{2}{\pi} V_s \sin(\omega t) \tag{17}$$

$$I_x = n\pi N I_{\text{op}} \tag{18}$$

$$\omega_o = \frac{1}{\sqrt{L_r\left(C_r \| nN^2 C_{b,\text{eff}}\right)}} \tag{19}$$

$$Q = \frac{nN^2}{R_{\text{ac}}} \sqrt{\frac{L_r}{\left(C_r \| nN^2 C_{b,\text{eff}}\right)}}. \tag{20}$$

The transconductance gain from input dc voltage V_s to the output dc I_{op} is derived as

$$\frac{I_{\text{op}}}{V_s} = \frac{N}{2R_{\text{load}}\sqrt{1 + Q^2\left(\frac{\omega}{\omega_o} - \frac{\omega_o}{\omega}\right)^2}}. \tag{21}$$

To achieve the constant load current I_{op}, even with input voltage change from $V_{s,\max}$ to $V_{s,\min}$ and load tolerance change condition from $R_{\text{load},\max}$ to $R_{\text{load},\min}$, the operating frequency should be changed within the operating curve which is overlapped on the gain curve shown in Fig. 10. Finally, the resonant tank value L_r, C_r, and the transformer turn ratio N can be calculated from (21) and the gain curve.

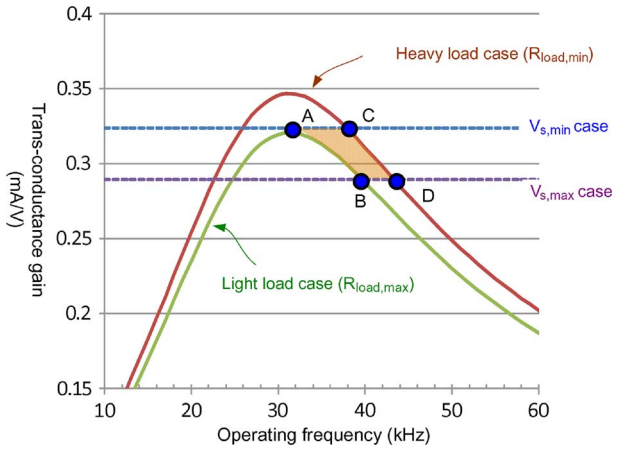

Fig. 10. Gain curve for design procedure.

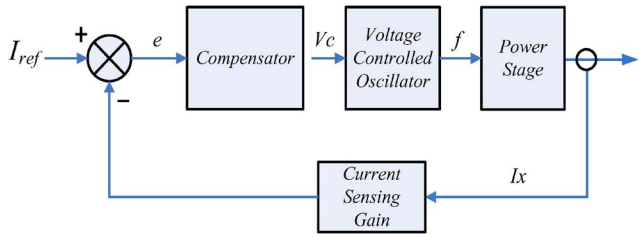

Fig. 11. Feedback control loop.

To obtain zero-voltage switching in the half-bridge switches, the operating frequency should be placed above the resonant frequency. Optimally, operating point A ($V_{s,\min}$, $R_{\text{load},\max}$) should be placed on the right side of the peak resonant point of the light load curve, as shown in the figure. Worst case efficiency degradation occurs in the operating point D ($V_{s,\max}$, $R_{\text{load},\min}$) where the operating frequency is far from the resonant frequency. In this case, a different Q design can reshape the sharpness of the curve and change the circulating current level in the resonant tank to improve the efficiency.

To achieve the current regulation, the total current in the secondary side is sensed and fed back to the frequency control loop, as in Fig. 11. A detailed compensator design for the frequency control loop is well established in other literature [17] and is out of the scope of this paper. The control loop regulates its total current for the all the LED channels by adjusting the operating frequency. When the input voltage increases, the operating frequency also increases to lower the transconductance gain in (21). The control scheme works well particularly for the different LED string forward voltages. If all the LED strings have the minimum forward voltage $V_{\text{op}}, \min$, the operating frequency is moving on the heavy load curve C-D according to the input voltage variation. If all the LED strings have the maximum forward voltage $V_{\text{op}}, \max$, the operating frequency is moving on the light load curve A-B. Usually, in mass production, LED strings with lower forward voltage are coexisting with those with higher forward voltage and the operating point moves inside the A-B-C-D area.

By using aforementioned procedure, a 100-W prototype balancing converter for six-channel $(n = 3)$ LED strings is designed, and its design values are listed in Table II. The input

TABLE II
MAJOR COMPONENT LISTS

Location	Description	Value	H/W Implementation	Size (Package)
C_1~C_6	balancing cap.	4.7nF	600V/film	12.5mm× 11.5mm×6mm
Cr	dc block cap.	1000nF	400V/film	17.5mm× 15mm×6mm
Lr	series inductor	1.3mH	EFD4549 (gapped)	45mm× 49mm×6mm
N	turn rato	1.2		
C_f	output cap.	22uF	250V/electrolytic	17mm×10pi
M_1,M_2	MOSFET	-	FDPF12N50	TO-220
D	rectifier	-	1N4007	DO-41

voltage range is 340–380 V that is supplied by a power factor correction stage, and the operating frequency is around 40 kHz. The target current in each LED string is set to 95 mA, and the allowable deviation is assumed to be 3%. In the following section, the performance of the proposed circuit is verified by simulation and hardware using this prototype.

VI. PERFORMANCE ESTIMATION

A. Statistical Analysis

As mentioned before, current deviation between any two branches $(n = 1)$ can be estimated by (3). However, in cases of more than two channels $(n > 1)$, such an equation-based analysis becomes very complex. In this case, statistical analysis is more powerful to estimate the performance of the balancing.

The LED string sample used in this paper consists of 54 white LED chips in series connection. Assuming that the individual LED chip forward voltage as a random variable with Gaussian distribution, probability theory [18] shows that the LED string forward voltage distribution is also Gaussian because the sum of random variables with Gaussian distribution also has Gaussian distribution.

To estimate overall balancing performance for multiple channels, simulation tools providing statistical worst case analysis can be used. In this paper, a Monte Carlo simulation has been performed using PSpice. In the simulation, the component values in Table II are used and balancing capacitors are assumed to be constant. The upper and lower limit values $R_{\mathrm{load,max}}$ (1.73 kΩ) and $R_{\mathrm{load,min}}$ (1.87 kΩ) are obtained using (14) and Table I; thus, the device tolerance parameter (DEV) is set to 3.9% for each equivalent load resistor. The number of trials is 50, and the distribution is assumed to be Gaussian.

The results are listed in Fig. 12, and the maximum deviation between the currents in each LED string is nearly 2.57 mA (2.7%). In real situations, because of the tolerance of other components, the current balancing can be worse than the estimation. Even in this case, the slightly decreased balancing capacitance value from the original calculation, which means increased reactance factor, can be adopted to enhance the current-balancing performance.

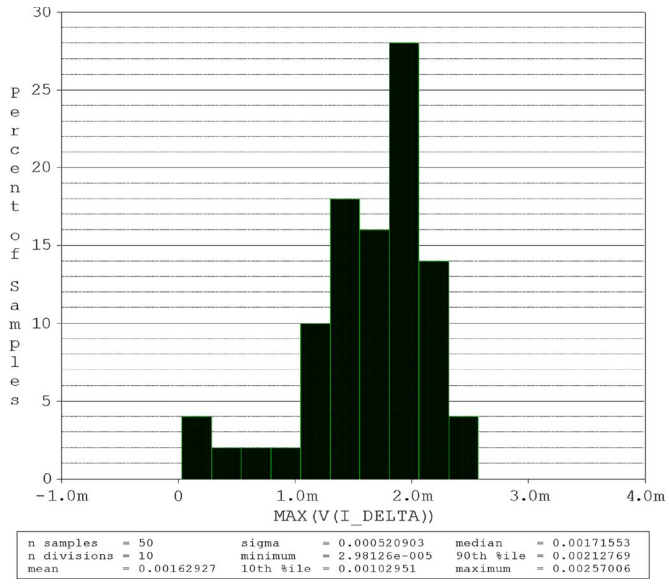

Fig. 12. Monte Carlo simulation using PSpice.

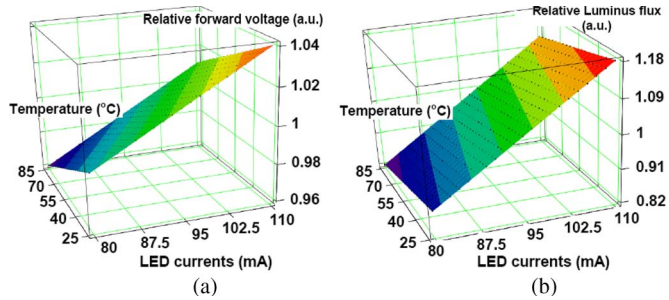

Fig. 13. Characteristics of the LED string sample. (a) Relative forward voltage. (b) Relative luminus flux.

B. Temperature Effects and Luminus Flux

Fig. 13 reconstructed the characteristics of the LED string sample based on the datasheet [19]. When the temperature of the LED string increases from 25 °C to 85 °C, the forward voltage of the LED string decreases by 4%; thus, all the forward voltage spreads shown Table I will be shifted to be in the range of 158–171 V. Even in this case, the balancing performance of the proposed scheme is almost unchanged. The upper and lower limit values in the high temperature are recalculated as $R_{\mathrm{load,max}}$ (1.66 kΩ) and $R_{\mathrm{load,min}}$ (1.80 kΩ) using (14), and the DEV remains unchanged to 3.9%; thus, the current-balancing performance is the same as before.

Fig. 13 also shows relative luminous intensity of LED string versus current. From the curve, 2.7% current deviation makes 3.0% deviation in luminous intensity.

VII. EXPERIMENTAL RESULTS

To verify the operation of the proposed circuit, a 100-W hardware prototype to drive six LED channels $(n = 3)$ is constructed using the designed value in Table II. The series inductance and the transformer were integrated into one component using the technique in [17]. The photographs of the hardware and LED backlight load have been shown in Figs. 14 and 15.

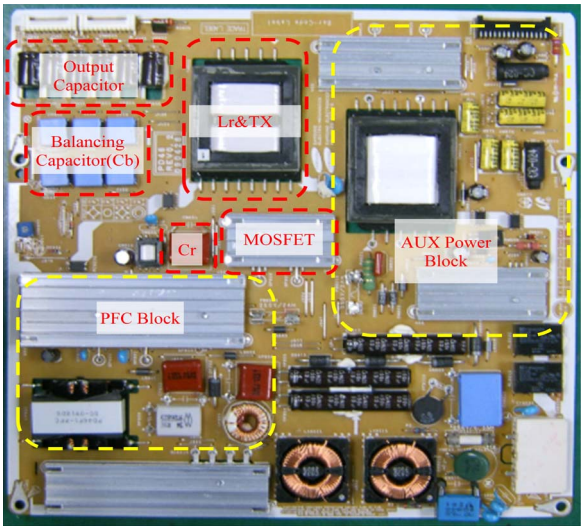

Fig. 14. Prototype hardware implementation.

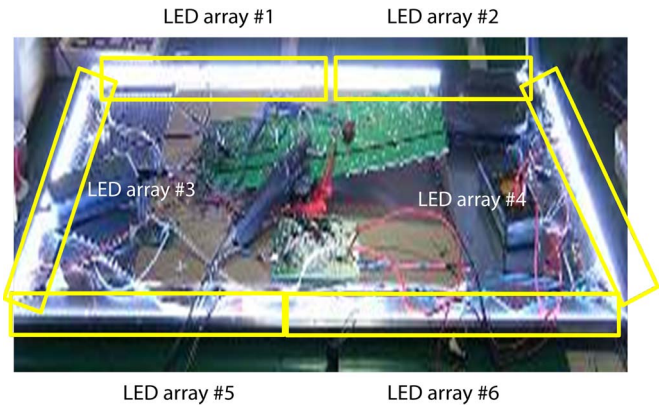

Fig. 15. LED backlight prototype hardware: edge configuration.

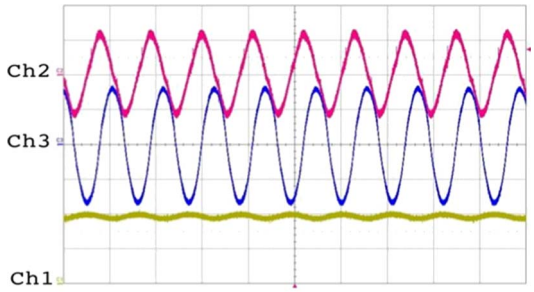

Ch2: Primary current (1A/div., 20us/div)

Ch3: Balancing capacitor voltage (350V/div.)

Ch1: DC blocking capacitor voltage (100V/div.)

Fig. 16. Experimental waveforms: Resonant current and voltage. (Ch2) Primary current (1 A/div, 20 μs/div). (Ch3) Balancing capacitor voltage (350 V/div). (Ch1) DC blocking capacitor voltage (100 V/div).

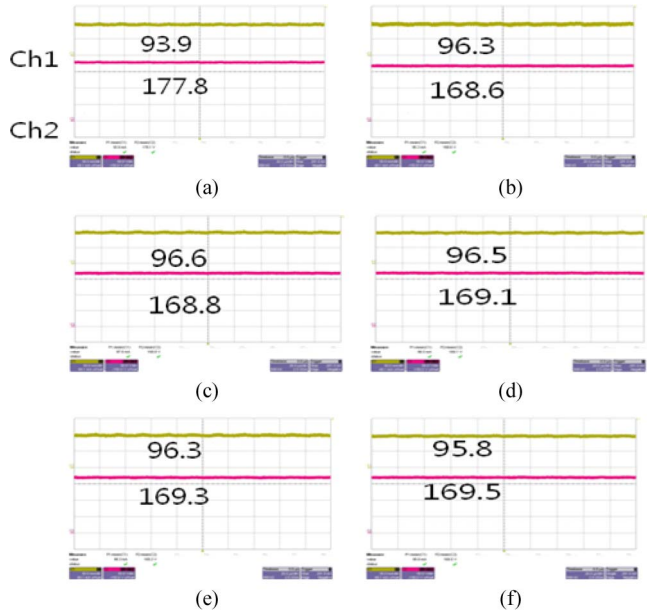

Ch1: LED Current(50mA/div.) Ch2: LED Voltage (50V/div.)

Fig. 17. Experimental waveforms: LED currents. (a) Channel #1. (b) Channel #2. (c) Channel #3. (d) Channel #4. (e) Channel #5. (f) Channel #6. (Ch1) LED current (50 mA/div). (Ch2) LED voltage (50 V/div).

TABLE III
SUMMARY OF THE MEASURED LED CURRENTS

Channel	LED string forward voltage (V)	Measured Current (mA)	Error (%)[a]
1	177.8	93.9	-1.16%
2	168.6	96.3	1.37%
3	168.8	96.6	1.68%
4	169.1	96.5	1.58%
5	169.3	96.3	1.37%
6	169.5	95.8	0.84%

[a] Deviation from the rated value of 95mA

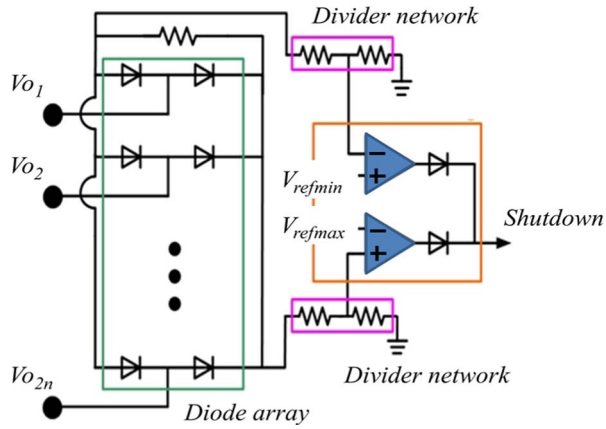

Fig. 18. Protection circuit for LED open/short condition.

Fig. 16 shows resonant tank waveforms. The secondary current loop regulates the total currents such that its current is maintained to be 3π times the individual LED current; thus, the circulating current in the primary-side resonant tank is about 1.2 A. As for the voltage stress, the proposed mechanism requires the balancing capacitor voltage to be as high as 550 V, which is a major resonant component. The primary series capacitor C_r operates as a dc blocking capacitor.

The presented experimental results in Fig. 17 are six-channel LED string currents and their forward voltages. The LED string loads are intentionally binned by its forward voltage such that channel #1 has the higher forward voltage of about 178 V

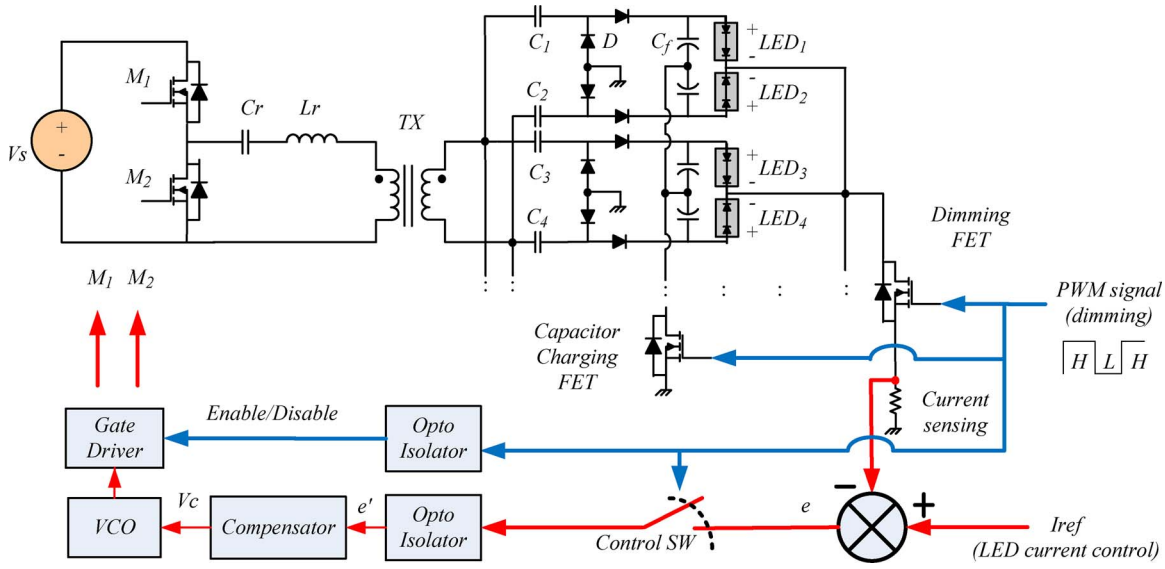

Fig. 19. Dimming scheme for the proposed circuit.

and the other five channels have the lower voltage of about 169 V. The measured load currents and balancing performance are summarized in Table III. Even with 9-V spread in forward voltages, the measured LED currents are balanced within 1.8% by our proposed scheme. It can be shown that, due to the inherent symmetry mentioned before, the partial sum of currents in the even branch and that of currents in the odd branch have almost the same value. The experimental results not only verify the underlying current-balancing principle but also show the performance of the proposed topology.

The measured efficiency of the proposed LED driving power stage is 93.4%. The overall system efficiency is about 85.5%, which includes a power-factor-correction preregulator having an efficiency of 90.9% and an auxiliary 4.2-W flyback power stage for drive and control circuitry.

VIII. Protection Scheme

In the proposed circuit, without a protection scheme, when one LED string is open or short, the current-balancing performance can be seriously degraded. There are three cases in the fault scenario.

Case 1) LED string short.
Case 2) LED chip short.
Case 3) LED string or LED chip open.

Case 1 may happen when the cathode line and the anode line of the string are accidentally short. In this case, the impedance of that branch is very low, the current in that branch increases too much beyond the current-balancing specification, and the output diodes may be destroyed by the overcurrent condition. Case 2 means the LED forward voltage decreases by one LED chip voltage. The current in that branch slightly increases, and the increment can be calculated by (1). If the resulting LED forward voltage reduction is out of the range in Table I, the current-balancing performance becomes poor. Case 3 occurs when the electrical paths to the LED string are lost or LED chips are accidentally damaged to open. Case 3 increases the output capacitor voltage with no current discharging path and may destroy the capacitor.

In the backlight system, the overall circuit operation should be disabled in the fault scenario, because any of the aforementioned scenarios will not guarantee uniform backlight brightness. To handle it, the protection method in Fig. 18 is suggested. The output filter capacitor voltage $Vo_1 - Vo_{2n}$ for each LED string is sensed, the highest and the lowest voltage are continuously monitored through the diode arrays, and they are compared with the minimum and maximum threshold voltages $V_{\mathrm{ref,min}}$ and $V_{\mathrm{ref,max}}$. If any capacitor voltage is below the minimum threshold (Case 1 or 2) or above the maximum threshold (Case 3), the protection logic shuts down all the backlight systems.

IX. Dimming Scheme

The dimming function which changes the brightness of the display is another essential feature of backlight units. In case of LED backlight systems, pulsewidth-modulation (PWM) dimming is preferred over analog dimming. With PWM dimming excited by a low-frequency reference signal of 100–200 Hz, the peak current is held constant and variations in white balance or color spectrum shift are minimized throughout the dimming range [20].

In the proposed balancing circuit, PWM dimming is not easily implemented by the enabling and disabling of the gate pulse of the half bridge. Because of the discharging of the output capacitor (Cf), even when the PWM signal changes from high to low and the half bridge stops switching on and off, the LED current does not go to zero instantly. The current slowly decays as the capacitor voltage discharges until the PWM signal toggles to high, which makes a poor dimming performance.

To provide elaborate PWM dimming, a MOSFET switch (FQU13N50L) has been placed between the cathodes of LED strings and the total current sensing resistor as in Fig. 19. The dimming FET provides global dimming—all the LED arrays

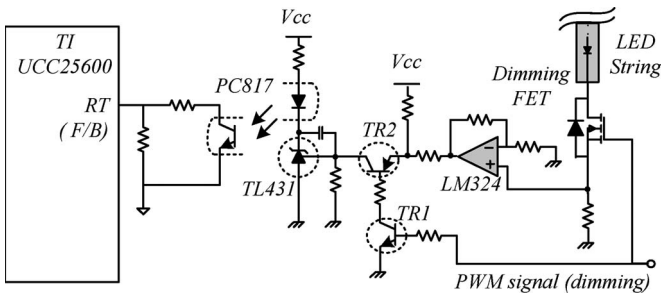

Fig. 20. Dimming control circuit.

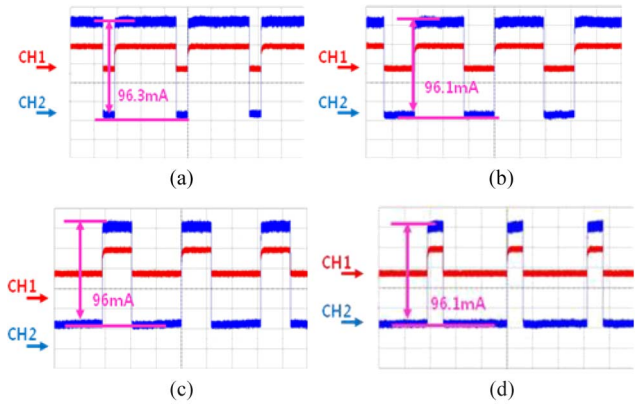

Ch1: PWM reference(5V/div.) Ch2: LED current (20mA/div.)

Fig. 21. Dimming waveforms with various PWM duty cycles. (a) 84%. (b) 62%. (c) 37%. (d) 20%. (Ch1) PWM reference (5 V/div). (Ch2) LED current (20 mA/div).

turn on and off at the same time according to the PWM signal. The stored voltage in the output capacitor does not find a path to discharge through the LED; thus, the LED current never flows during the off period.

When the frequency control scheme in Fig. 11 is applied to the dimming scheme, the feedback compensator can be saturated when the PWM signal is low because the operating frequency moves to its minimum achievable value and the transconductance gain increases. This control loop behavior generates turn-on transient spikes on the LED current. To alleviate the deep saturation effect, a dimming control circuit as in Fig. 20 has been adopted. When the PWM signal goes to low, TR1 turns off TR2 and temporarily breaks the feedback control loops. The compensator (TL431) without feedback loop makes the operating frequency stay near the present value and not to go far to the minimum value as before. At the same time, a capacitor-charging FET (FQU13N50L) in Fig. 19, which has been placed between the common negative nodes of the output filter capacitors and ground, turns off to prevent the output capacitor from charging. When the PWM signal becomes high, TR2 turns on and the capacitor charging FET is turned on again.

To verify the new scheme, this circuit has been merged into the prototype hardware. Fig. 21 shows LED current waveforms with respect to PWM signal. During the dimming function, the current value is held nearly constant such that the overall current-balancing performance is maintained.

X. Conclusion

In this paper, a new current-balancing driver circuit for LED backlight systems has been proposed. A smart combination of an inherent symmetry of circuit and capacitive balancing mechanism enables an efficient and cost-effective current balancing. A detailed analysis of the operating principle is performed to generalize the proposed scheme, thus showing that the balancing performance can be finely adjusted by the reactance factor. A PWM dimming scheme and a protection method are also presented. The experimental results of a 100-W six-channel LED backlight system verify the feasibility of the proposed balancing and dimming scheme.

Acknowledgment

S. Choi would particularly like to thank P. Agarwal for his help during this work.

References

[1] C. G. Kim, K. C. Lee, and B. H. Cho, "Analysis of current distribution in driving multiple Cold Cathode Fluorescent Lamps (CCFL)," *IEEE Trans. Ind. Electron.*, vol. 54, no. 1, pp. 365–373, Feb. 2007.
[2] S. Yang, S. Lee, H. Kim, H. Lee, H. Mok, and G. Choe, "A new current balancing methods of CCFL for LCD TV backlight," in *Proc. IEEE Power Electron. Spec. Conf.*, 2006, pp. 1–5.
[3] X. Jin, "Balancing transformers for ring balancer," U.S. Patent 7 294 971, Nov. 13, 2007.
[4] H. van der Broeck, G. Sauerlander, and M. Wendt, "Power driver topologies and control schemes for LEDs," in *Proc. IEEE Appl. Power Electron. Conf.*, 2007, pp. 1319–1325.
[5] Y. Hu and M. M. Jovanovic, "A novel LED driver with adaptive drive voltage," in *Proc. IEEE Appl. Power Electron. Conf.*, 2008, pp. 565–571.
[6] H. Chiu and S. Cheng, "LED backlight driving system for large-scale LCD panels," *IEEE Trans. Ind. Electron.*, vol. 54, no. 5, pp. 2751–2760, Oct. 2007.
[7] S. Lee, H. Kim, J. Kwon, C. Lee, M. Choi, and B. Oh, "New design of integrated power and integrated driver with LED module (IP-IDLM) driving system for LED backlight in LCD," in *Proc. IEEE Int. Symp. Ind. Electron.*, 2007, pp. 584–587.
[8] C. Wu, T. Wu, J. Tsai, Y. Chen, and C. Chen, "Multistring LED backlight driving system for LCD panels with color sequential display and area control," *IEEE Trans. Ind. Electron.*, vol. 55, no. 10, pp. 3791–3800, Oct. 2008.
[9] Y. Lo, K. Wu, K. Pai, and H. Chiu, "Design and implementation of RGB LED drivers for LCD backlight modules," *IEEE Trans. Ind. Electron.*, vol. 56, no. 12, pp. 4862–4871, Dec. 2009.
[10] S. M. Baddela and D. S. Zinger, "Parallel connected LEDs operated at high frequency to improve current sharing," in *Conf. Rec. IEEE IAS Annu. Meeting*, 2004, pp. 1677–1681.
[11] S. Choi, P. Agarwal, T. Kim, J. Yang, and B. Han, "Symmetric current balancing circuit for multiple DC loads," in *Proc. IEEE Appl. Power Electron. Conf.*, 2010, pp. 512–518.
[12] M. Nishikawa, Y. Ishizuka, H. Matsuo, and K. Shigematsu, "An LED drive circuit with constant-output-current control and constant-luminance control," in *Proc. IEEE INTELEC*, 2006, pp. 1–6.
[13] M. Doshi and R. Zane, "Digital architecture for driving large LED arrays with dynamic bus voltage regulation and phase shifted PWM," in *Proc. Appl. Power Electron. Conf.*, 2007, pp. 287–293.
[14] C. Chen, C. Wu, and T. Wu, "Fast transition current-type burst-mode dimming control for the LED back-light driving system of LCD TV," in *Proc. PESC*, 2006, pp. 1–7.
[15] M. Khatib, "Ballast resistor calculation—Current matching in parallel LEDs," Texas Instrument, Dallas, TX, Application Rep. SLVA325, 2009.
[16] M. K. Kazimierczuk and D. Czarkowski, *Resonant Power Converters*. New York: Wiley, 1995.
[17] E. X. Yang, F. C. Lee, and M. Jovanovic, "Small-signal modeling of series and parallel resonant converters," in *Proc. IEEE Appl. Power Electron. Conf.*, 1992, pp. 785–792.
[18] A. Papoulis, *Probability, Random Variables and Stochastic Processes*. New York: McGraw-Hill, 1991.

[19] *LBU46MFAE7 Specifications*, Samsung Electro-Mechanics Co., Suwon, Korea, Feb. 2009.
[20] B. Yang, "Topology investigation for front end DC/DC power conversion for distributed power system," Ph.D. dissertation, Virginia Tech, Blacksburg, VA, Sep. 2003.
[21] W. Lun, K. H. Loo, S. Tan, Y. M. Lai, and C. K. Tse, "Bilevel current driving technique for LEDs," *IEEE Trans. Power Electron.*, vol. 24, no. 12, pp. 2920–2932, Dec. 2009.

Sungjin Choi (M'05) was born in Seoul, Korea, in 1973. He received the B.S., M.S., and Ph.D. degrees in electrical engineering from Seoul National University, Seoul, in 1996, 1998, and 2006, respectively.

From 2006 to 2008, he was a Research Engineer with Palabs Company, Ltd., Seoul. From 2008 to 2011, he was with Samsung Electronics Company, Ltd., Suwon, Korea, as a Senior Research Engineer and Principal Research Engineer, developing drive circuits for liquid-crystal-display systems. In 2011, he joined the University of Ulsan, Ulsan, Korea, where he is currently an Assistant Professor with the School of Electrical Engineering. His research interests include component modeling, topology and control of high-frequency switching converters, and power electronics for renewable energy sources.

Taehoon Kim was born in Jeju Island, Korea, in 1981. He received the B.S. degree in electrical engineering from Dongguk University, Seoul, Korea, in 2006.

Since 2006, he has been a Research Engineer with Samsung Electronics Company, Ltd., Suwon, Korea, developing drive circuits for liquid-crystal-display systems. His research interests include dc–dc converters, ac–dc converters, and power supplies for light-emitting-diode lighting systems.